Influence of the Characteristics of γ-Aluminas on the Dispersion and the Reducibility of Supported Cobalt Catalysts

Rafeh Bechara,*,† David Balloy,† Jean-Yves Dauphin,‡ and Jean Grimblot§

Laboratoire de Génie Chimique et d'Automatique, ENSCL-ECLille, B.P.48, 59651 Villeneuve d'Ascq Cédex, France, Laboratoire de Mécanique et Matériaux, ECLille, B.P.48, 59651 Villeneuve d'Ascq Cédex, France, and Laboratoire de Catalyse Hétérogène et Homogène, URA CNRS 402, USTL, 59655 Villeneuve d'Ascq Cédex, France

Received October 14, 1998. Revised Manuscript Received April 30, 1999

Four commercial aluminas and different cobalt loadings have been selected to better understand the interactions between Co oxides and metallic cobalt with alumina surfaces. The solids have been characterized, after drying and calcination procedures or after reduction under H_2, using thermogravimetric analysis (TGA), X-ray diffraction (XRD), X-ray photoelectron spectroscopy (XPS), and scanning electron microscopy (SEM). The information has been complemented by specific surface area (SSA), porosimetry, and magnetic measurements. Both the effect of the cobalt content and the texture of supports have been examined. It appears that the cobalt reducibility is influenced by the cobalt loading and the alumina porosity mainly because of the heterogeneity in the Co distribution. Two cobalt reduction steps were identified. The first one which transforms Co_3O_4 into CoO appears to be easy from 500 K whereas the second one which produces metallic Co occurs in a wide range of temperatures (623−873 K) and is highly dependent on the support characteristics. The use of high specific surface area supports leads to catalysts with a good dispersion when their macroporosity (pore diameter $\phi > 0.05$ μm) is large. However, in all the cases, the grain edges of the powdered sample or the periphery of pellets are richer in cobalt than the bulk, and the cobalt is less dispersed. The reduction of cobalt oxide localized at the periphery is facilitated by its poor dispersion. On the other hand, the well-dispersed cobalt species in the core of the pellets are more strongly interacting with the support and are not so easily reduced.

Introduction

Cobalt-based catalysts are of interest in the field of heterogeneous catalysis from at least three points of view: (i) in the oxidized state they constitute active catalysts for total combustion of organic molecules;[1−3] (ii) in combination with Mo (or W) dispersed on alumina supports, they are precursors of sulfided catalysts active in hydrosulfurization;[4] (iii) after prereduction, they constitute excellent catalysts for CO hydrogenation to hydrocarbons (Fischer−Tropsch synthesis).[5−7] For the last application, other metals such as iron, ruthenium, or nickel can be used as well. Cobalt-based catalysts are particularly advantageous because they are relatively inexpensive and have a low water-gas shift activity.[8,9]

Many studies have been conducted about the effects of different preparation conditions on the catalyst's properties. Various supports for cobalt including silica, alumina,[10,11] kieselguhr, zeolite,[11] titania, carbon, and magnesia[12] have been used to improve metal dispersion and attrition resistance. The catalysts exhibit a wide range of properties such as specific surface area, porosity, acidity, and catalytic performances.[13,14]

Some supports may have strong interactions with the active phase or with its precursor. For Co/Al_2O_3 catalysts, cobalt ion diffusion into the structure of alumina leads to species that are difficult to reduce.[11,15−19]

† Laboratoire de Génie Chimique et d'Automatique.
‡ Laboratoire de Mécanique et Matériaux.
§ Laboratoire de Catalyse Hétérogène et Homogène.
* Corresponding author: Fax 00.33.3.20.33.54.44; E-mail bechara@eclille.fr.

(1) McCarty, J. C.; Quinland, M. A.; Wise, H. *Proc. 9th Int. Congr. Catal.* **1988**, 1818.
(2) Machida, M.; Eguchi, K.; Arai, H. *J. Catal.* **1989**, *120*, 377.
(3) Ozkan, U. S; Kueller, R. F.; Moctezuma, E. *Ind. Eng. Chem. Res.* **1990**, *29*, 1136.
(4) Topsoe, H.; Clausen, B. S.; Massoth, F. E. *Hydrotreating Catalysis*; Springer-Verlag: Berlin, 1996 and references therein.
(5) Blanchard, M.; Canesson, P.; De Werbier, P.; Chami, J. *Proc. 9th Int. Congr. Catal.* **1988**, 767.
(6) Vanhove, D.; Zhuyong, Z.; Makambo, L.; Blanchard, M. *Appl. Catal.* **1984**, *9*, 327.
(7) Iglesia, E.; Reyes, S. C.; Madon, R. J.; Soled, S. L. *Adv. Catal.* **1993**, *39*, 221.
(8) Anderson, R. B. In *Catalysis;* Emmett, P. H., Ed.; Reinhold: New York, 1956; Vol. 5, p 1.
(9) Goodwin, J. G. *ACS Prepr. Symp.* **1991**, *36* (1), 156.
(10) Schanke, D.; Vada, S.; Blekkan, E. A.; Hilmen, A. M.; Hoff, A.; Holmen, A. *J. Catal.* **1995,** *156*, 85.
(11) Bessell, S. *Appl. Catal.* **1993**, *96*, 253.
(12) Reuel, R. C.; Bartholomew, C. H. *J. Catal.* **1984**, *85*, 78.
(13) Zowtiak, J. M.; Bartholomew, C. H. *J. Catal.* **1983**, *83*, 107.
(14) Lepage, J. F.; Cosyns, J.; Courty, P.; Freund, E.; Franck, J. P.; Jacquin, Y.; Juguin, B.; Marcilly, C.; Martino, G.; Miquel, J.; Montarnal, R.; Sugier, A.; Van Landeghem, H. *Catalyse de contact*; Editions Technip: Paris, 1978.
(15) Van't Blik, H. F. J.; Prins, R. *J. Catal.* **1986**, *97*, 188.

10.1021/cm981015n CCC: $18.00
Published on Web 06/24/1999

Crystallites of cobalt oxide of small size are generally influenced by such interactions with the support.[15,20−22]

In this study, a systematic investigation of the metal loading and of the texture of the alumina support on the cobalt dispersion and distribution in the particles and their effects on the reducibility of the oxide precursors to conduct to the metallic Co phase was performed by means of various techniques. In a following paper,[23] the characteristics will be correlated with the performance of the catalysts for the conversion of syngas.

Experimental Section

Catalysts Preparation. The catalysts were prepared by the incipient wetness method. Four commercial γ-aluminas were used in the form of powder (from Aldrich, reference support A) or as spherical pellets (from Rhône-Poulenc, the supports CR3S, Grad D, and SCM200T, hereafter named supports C, G, and S, respectively). They were impregnated with an aqueous solution of cobalt nitrate hexahydrate (Janssen Chemica). About 15−17 wt % of Co was deposited on the four aluminas with the aim to study the effects of the support. In addition, the influence of the metal loading was studied with six catalysts prepared from supports A and S and impregnated with about 9, 16, and 25 wt % Co.

After impregnation, the solids were dried at 383 K for one night and calcined in air at 783 K (heating rate: 5 K/min) for 3 h, with a 30 min break at 473 K to make the decomposition of the precursor more easy. The solids in the oxide form were also reduced under hydrogen (2.5 L/h) for 15 h at different temperatures (heating rates are respectively 5 and 1 K/min for the last 100 deg), which corresponds to WHSV between 800 and 1200 h^{-1}.

Texture Characterization. Specific surface areas (SSA) of supports and catalysts were determined by nitrogen adsorption at 77 K using a Quantasorb Jr. sorptometer and the single-point BET method. Total pore volume (TPV) and pore size distributions were determined by mercury porosimetry. Data concerning supports C, G, and S were provided by Rhône-Poulenc, and the porosity of alumina A was determined at the "Institut Français du Pétrole" (IFP).

Thermogravimetric Analysis (TGA). The sample weight loss during temperature increase from 293 to 1073 K (heating rate: 1 K/min), in flowing air or H_2, was measured with an electronic ultramicrobalance (Sartorius 4102). A 40−50 mg sample was heated in a quartz crucible under a 2.5 L/h gas flow. The weight loss rate was represented by the derivative curve of the thermogravimetric evolution. The degree of cobalt reduction (R) was calculated from the weight loss of the catalysts in flowing H_2 after correction of the support contribution which desorbs some molecules (water or products of hydrogenation of carbonaceous deposits) during the heating procedure.

X-ray Diffraction (XRD). X-ray powder diffraction patterns were recorded with a Siemens K710 diffractometer using the Co Kα radiation (λ = 0.1789 nm) and a scanning rate of 0.02 deg/s. The EVA 3.10 software was used to subtract the Kα_2 X-ray contribution and to smooth the diagrams. The cobalt phases have been identified by comparison with the JCPDS database, and average crystallite sizes (d_m) have been calculated according to the Scherrer equation.[24]

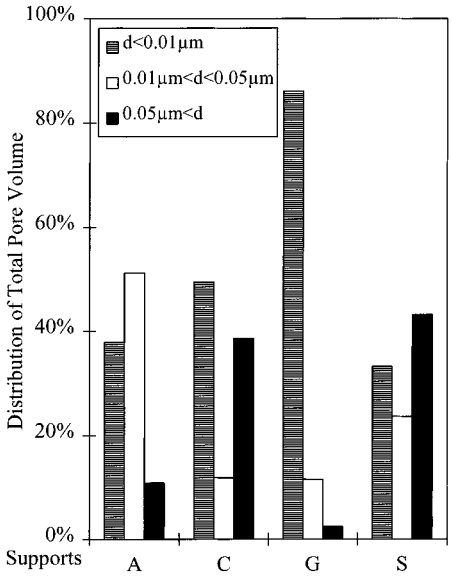

Figure 1. Pore size distribution of supports.

Table 1. Texture of Supports

support	SSA (m^2/g)	TPV (mL/g)	form and main size
A	56	0.22	powder 200 μm
C	332	0.55	pellets 4−6 mm
G	315	0.45	pellets 2−4 mm
S	150	0.72	pellets 2−4 mm

Scanning Electron Microscopy (SEM). Supports and catalysts observation was conducted with a Hitachi reflection electron microscope. Pictures by secondary and backscattered electrons were obtained with a magnification between ×50 and ×7000. The X-ray emission analyses were performed to determine the local atomic compositions.

X-ray Photoelectron Spectroscopy (XPS). XPS spectra of catalysts were obtained with the use of a Kratos AEI ES 200B spectrometer, equipped with an Al anode (1486.6 eV). All samples were crushed as a fine powder and thinly spread on an indium plate. It is therefore inferred that the XPS analyses of the extrudates are averaged between all the grains. Variation of composition between the external surface and the core of the pellets cannot be provided by this method. Binding energy (BE) was referenced to the C 1s line at 284.8 eV.

The XPS intensity ratios I_{Co}/I_{Al} were calculated from the Co $2p_{1/2-3/2}$ and Al 2p peak area, respectively. When plotting this ratio as a function of the Co amount expressed as the number of Co atoms deposited per surface area unit (nm^2) of the final catalyst, changes of the Co distribution within the series of prepared solids can be found.

Magnetic Measurements. The magnetic measurements were carried out by an axial extraction technique.[25] The sample magnetization was measured at different magnetic fields between 0 and 21 kOe. The saturation magnetization (M_s) was obtained by extrapolating magnetization to infinite magnetic field. As M_s is proportional to the mass of metallic cobalt in the sample, the degree of reduction was calculated after calibration with pure cobalt.

Results and Discussion

Supports. The main textural characteristics of the supports are reported in Table 1 and Figure 1. The lowest specific surface area (SSA) was that of the powdered support A while supports C and G exhibit SSA

(16) Martens, J. H. A.; Van't Blik, H. F. J.; Prins, R. *J. Catal.* **1986**, *97*, 200.
(17) Van't Blik, H. F. J.; Koningsberger, D. C.; Prins, R. *J. Catal.* **1986**, *97*, 210.
(18) Goodwin, J. G.; Chen, Y. W.; Chuang, S. C. In *Catalytic Conversion of Synthesis Gas and Alcohols for Chemicals*; Herman, R. G., Ed.; Plenum Pub. Co.: New York, 1984; p 179.
(19) Dimitrova, P. G.; Mehandjiev, D. R. *J. Catal.* **1994**, *145*, 356.
(20) Zslodos, Z.; Hoffer, T.; Guczi, L. *J. Phys. Chem.* **1991,** *95*, 798.
(21) Chin, R. L.; Hercules, D. M. *J. Phys. Chem.* **1982**, *86*, 360.
(22) Ali, S.; Chen, B.; Goodwin, J. G. *J. Catal.* **1995**, *157*, 35.
(23) Bechara, R.; Balloy, D.; Vanhove, D., to be published.
(24) Cullity, B. D. *Elements of X-ray Diffraction*; Addison-Wesley Publishing Company: London, 1978.
(25) Dalmon, J. A. *Les techniques physiques de l'étude des catalyseurs*; IRC−CNRS, Editions Technip: Paris, 1988; p 791.

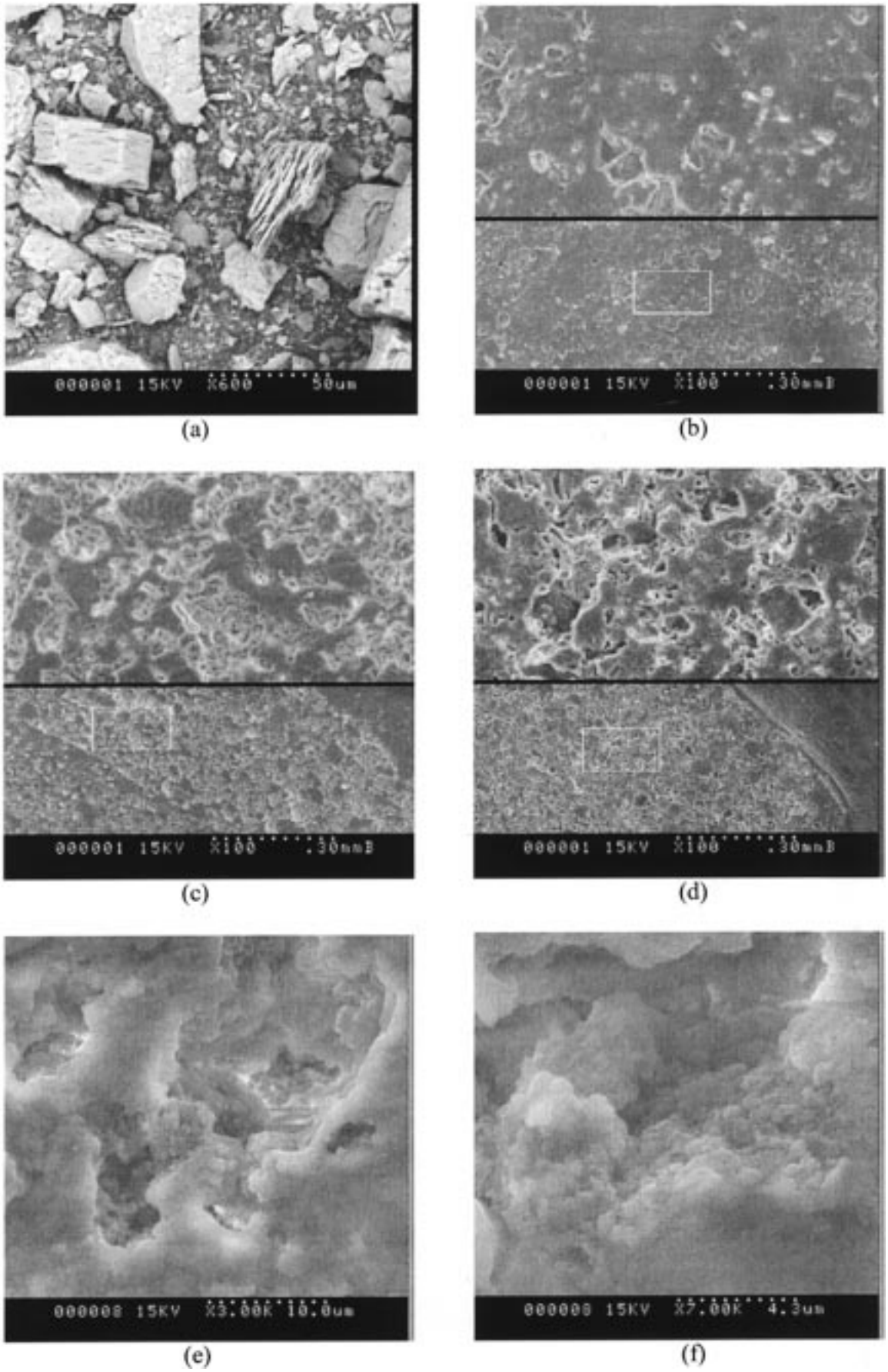

Figure 2. SEM pictures of the four alumina supports (a) support A (×600); (b) to (d), with a magnification ratio of ×100 at the bottom and ×500 at the top, middle of pellet respectively of G, C, and S alumina; (e) cavity of support C (×3000); (f) cavity of support C (×7000).

around 330 $m^2\ g^{-1}$. The total pore volume (TPV) range is between 0.22 and 0.72 $cm^3\ g^{-1}$. [The pore size distribution (Figure 1) appears quite different among the four supports considered.] Support G has the largest proportion of small pores with a diameter ϕ less than 0.01 μm.

The SEM pictures (Figure 2) qualitatively confirm the pore size distribution results. For supports A and G (Figure 2a,b), porosity is almost completely composed of mesopores, the diameter of which is less than 0.05 μm.[26] Aluminas C and S have a large fraction of macropores (ϕ > 0.05 μm) which are easily identified on SEM pictures (Figure 2c,d). The high magnification pictures (Figure 2e,f) show some small grains which cover the interior of the alumina cavities and develop a high specific Co area.

Impregnation and Precursor Decomposition. To investigate the effect of the support morphology on the impregnation and decomposition of the cobalt salt, TGA experiments have been performed on two samples having about the same Co loading (~14.9 and 16.9 wt %, respectively). The first sample (A2) was obtained with the powdered support while the second tested sample (S2) was obtained with pellets S.

The TGA curves (see Figure 3) show quite different results. Several steps can be easily identified on the A2 calcination curve. They correspond to the decomposition of the cobalt precursor ($Co(NO_3)_2 \cdot 6H_2O$) as given by the following sequence:[15,27]

$$\underset{\text{pink}}{Co(NO_3)_2.6H_2O} \xrightarrow{328K} \underset{\text{red}}{Co(NO_3)_2.3H_2O} \xrightarrow{373K} \underset{\text{purple}}{Co(NO_3)_2}$$

$$\xrightarrow{423-473K} \underset{\text{black}}{Co_3O_4\ (CoO)} \xrightarrow{1073K} \underset{\text{blue}}{CoAl_2O_4}$$

The first two steps mainly concern water removal while the next one implies decomposition of the nitrate ions. The transformation of CoO into cobalt aluminate in the high-temperature range does not induce weight loss. We conclude that after impregnation and drying cobalt deposited on the powdered support A remains as hexahydrated Co nitrate.

On the other hand, the single step up to 473 K of the S2 thermogravimetric curve indicates that part of the water is already removed from the $Co(NO_3)_2 \cdot 6H_2O$ during the impregnation−drying procedure. Indeed, as reported by Marcilly and Franck,[28] the drying−impregnation of porous pellets is exothermic and can initiate a dehydration that occurs at relatively low temperature. Moreover, the color of the S2 catalyst after impregnation tends to be purple, the color of dehydrated $Co(NO_3)_2$.[15,27] This information confirms that the cobalt solution−alumina interaction is effectively dependent on the morphology of the support.

Catalysts in the Oxidic State. The main textural and structural characteristics of the catalysts after calcination are reported in Table 2. In principle, impregnation of alumina by salts of metals that give supported oxides of rather high density (i.e., higher than the alumina density) naturally provokes a decrease of the specific surface area simply by a dilution effect. In Table 2, to estimate the importance of this "dilution", the measured specific surface area of the calcined catalysts and the theoretical contribution of the support are reported alone. On samples prepared with support A, there is a rather good correlation between the measured values and the expected contribution of the support. This means that porosity of the support is not affected by Co oxide deposition, and moreover, cobalt oxide does not develop its own porosity. By contrast, in C2 and G2 catalysts, the small pores are probably filled by Co oxide as the measured specific surface area values are considerably smaller than the pure support, and the dilution effect cannot explain this decrease. Indeed, other authors have also observed the blocking of the smallest pores when they are impregnated with cobalt.[11,19,29] The results obtained with samples of support S seem to indicate that the support porosity is not affected by Co deposition and that the cobalt oxide has a significant contribution to the measured surface area.

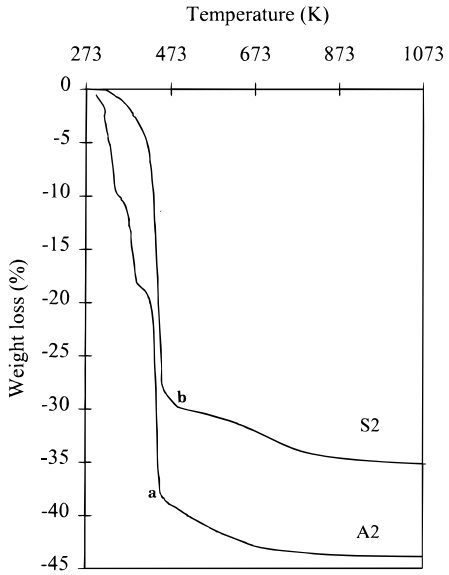

Figure 3. Thermogravimetric evolution of catalysts A2 (a) and S2 (b) during calcination after support impregnation.

The XRD patterns of calcined series A catalysts show the characteristic diffraction peaks of Co_3O_4 (Figure 4). Similar patterns are obtained for catalysts C2, G2, and S2: only the full widths at half-maximum ($\Delta_{1/2}$) of the peaks are different. This means that the average crystallite sizes (d_m) of the Co oxide particles, calculated from $\Delta_{1/2}$ using the Scherrer equation and reported in Table 2, depend on both the support origin and the Co loading.

For the catalyst series A and S, the crystallite size grows as the cobalt loading increases. Co_3O_4 dispersion seems to be better when the specific area of the support is high, as for catalysts of series S. Nevertheless, d_m is very important for catalyst G2 although the specific surface area of alumina G is high. Thus, the pore size distribution of support must be taken into account; the catalysts prepared from supports with macroporosity (S,

(26) Allen, T. *Particle Size Measurement*; Chapman and Hall: London, 1997; Vol. 2.
(27) *Handbook of Chemistry and Physics*, 66th ed.; CRC Press: Boca Raton, FL, 1985−1986.
(28) Marcilly, C.; Franck, J. P. *Revue de l'IFP* **1984**, *39*, 337.
(29) Bessell, S. *Appl. Catal. A* **1995**, *126*, 235.

Table 2. Cobalt Content, Specific Surface Area, and XRD Crystallite Average Sizes of Co−Alumina Catalysts

support	A			C	G	S		
catalyst	A1	A2	A3	C2	G2	S1	S2	S3
cobalt content (wt %)	8.5	14.9	26.3	16.8	17.1	9.8	16.9	25.4
specific surface area (m^2/g)[a]	55	42	36	170	180	148	138	120
support contribution (m^2/g)[b]	49.5	45	36	256	241	130	115	98
d_m (nm)[c]	21	23.5	34	13	34	10	11.5	13

[a] After calcination. [b] Theoretical contribution of the support which is diluted with a given amount of Co oxide. [c] Mean diameter of Co_3O_4 crystallite as determined by XRD (Scherrer equation).

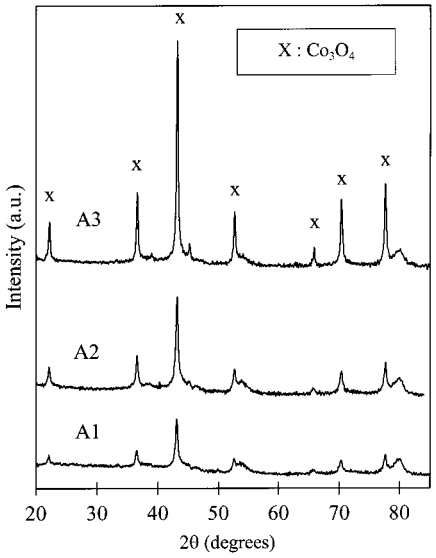

Figure 4. Influence of the cobalt loading on the XRD patterns of Co/Al_2O_3 catalysts (series with support A).

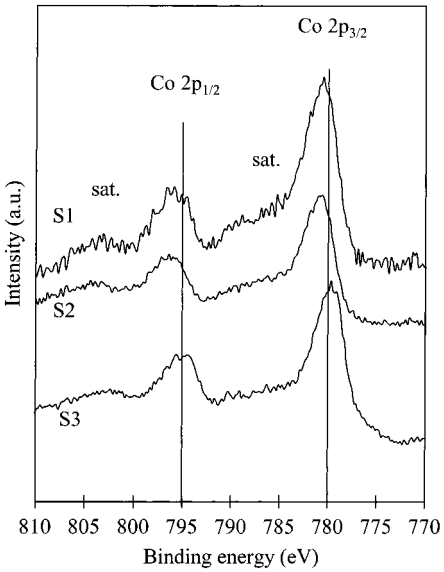

Figure 5. Influence of the cobalt loading on the XPS spectra of Co/Al_2O_3 catalysts (series with support S).

C) show smaller sizes for the deposited Co oxide particles (i.e., better cobalt dispersion).

X-ray photoelectron spectroscopy gives information about the chemical state of the cobalt species and their distribution on the surface of the catalysts particles. The influence of the cobalt content on the XPS binding energy of Co is presented in Figure 5. The spectrum of catalyst S3 is similar to that of pure Co_3O_4 : the $Co2p_{1/2}$ and $Co2p_{3/2}$ binding energies are 795 and 780 eV, respectively, and on the high binding energy sides, the shake-up satellite structure is not very intense. When

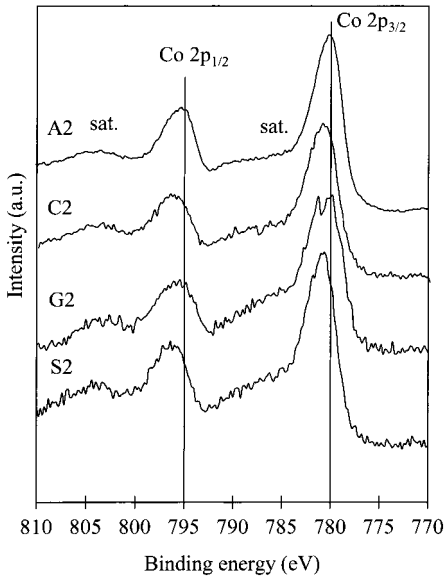

Figure 6. Influence of the support on the XPS spectra of Co/Al_2O_3 catalysts.

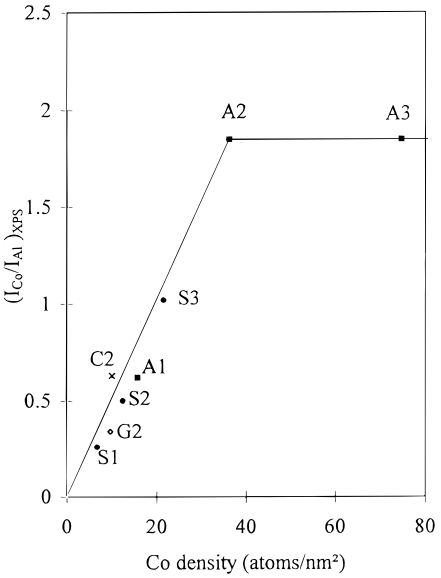

Figure 7. Variation of the intensity ratio $(I_{Co}/I_{Al})_{XPS}$ as a function of the cobalt density of the catalysts after calcination.

the cobalt content decreases (samples S2 and S1), the shift of binding energies to higher values indicates the presence of surface Co^{2+} species.[19,30] For catalysts of series A, the shift to higher binding energy is only observed in the case of sample A1. These Co^{2+} species may result in the formation of CoO instead of Co_3O_4 or in Co aluminate. As indicated in the sequence of

(30) Grimblot, J.; Bonnelle, J. P.; Beaufils, J. P. *J. Electron Spectrosc. Relat. Phenom.* **1976**, *8*, 437.

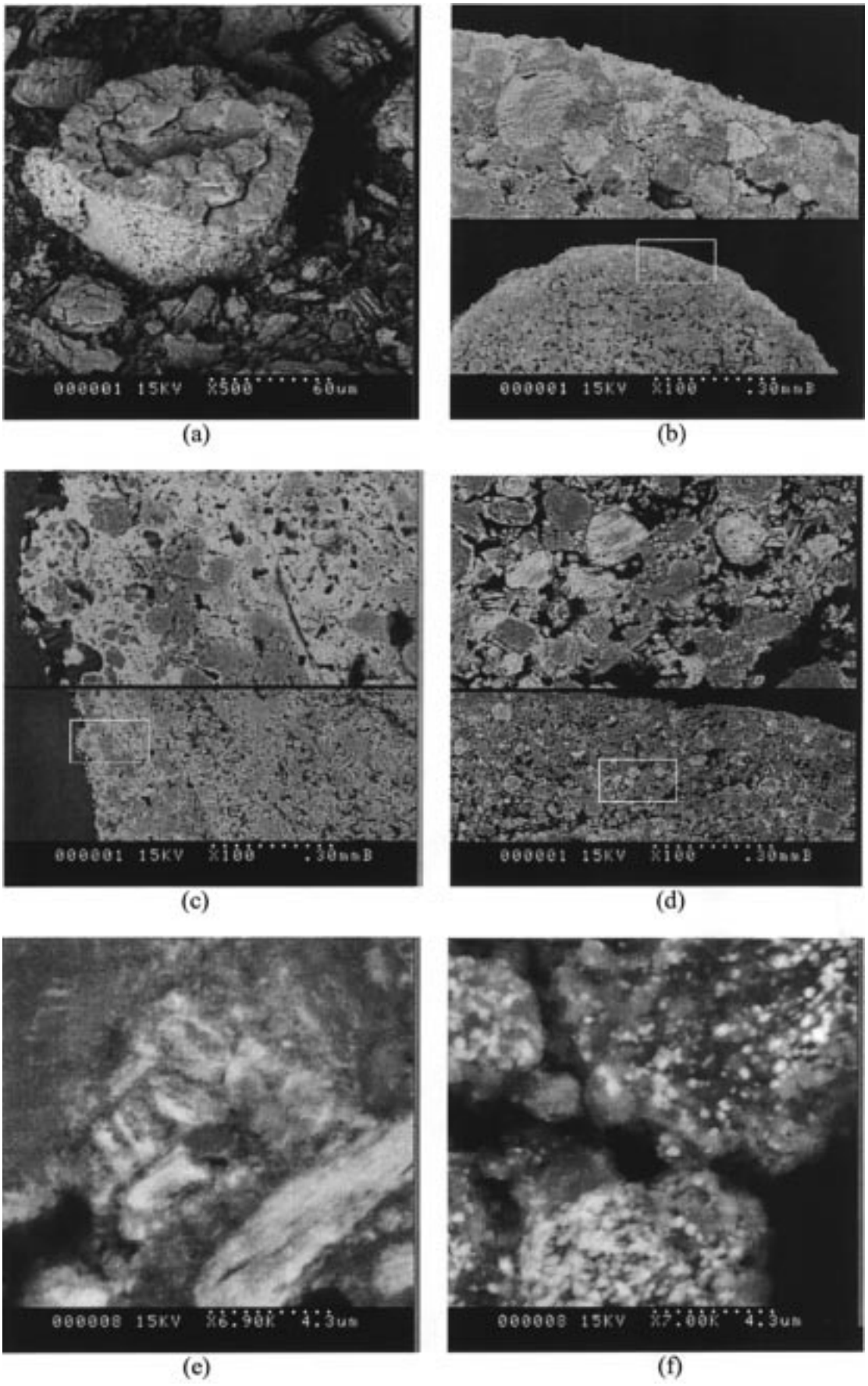

Figure 8. SEM pictures of four catalysts: (a) cut of a grain of catalyst A2 (×500); (b) to (d), with a magnification ratio of ×100 at the bottom and ×500 at the top, cut of a pellet respectively of G2, S2, and C2 catalyst; (e) cobalt at the border of the catalyst C2 (×7000); (f) cobalt at the core of the catalyst C2 (×7000).

decomposition of the Co precursor, Co_3O_4 is preferably formed under the calcination conditions used. However, for low Co content, the interaction of the Co species with the free alumina surface is favored, resulting in formation of bulk Co aluminate by Co^{2+} diffusion into the alumina framework depending on the alumina reactivity and temperature of calcination. Reduction of surface or bulk Co^{2+} species is more difficult than that of Co_3O_4 in accordance with the higher interaction with the support.[15,31−37] At the lowest Co loading, formation of surface or bulk Co aluminate is therefore preferred to CoO, the diffraction pattern of which has not been detected (Figure 4).The Co species which are not strongly interacting with alumina are forming crystallites of Co_3O_4 of small size as indicated in Table 2. Likewise, for the catalysts containing about 16 wt % Co and prepared with the supports that develop the highest specific area (C2, G2, S2), Co^{2+} ion formation by interaction with the support is easier than for catalyst A2 as observed in Figure 6.

The intensity ratio of XPS Co 2p and Al 2p peaks, which reflects the concentration of Co and Al atoms within the sample analyzed depth, allows to follow the evolution of the cobalt distribution at the catalysts surface when plotted as a function of the cobalt density (Figure 7). The linear evolution of the ratio $(I_{Co}/I_{Al})_{XPS}$ observed for catalysts S1 to A2 corresponds to a gradual coverage of the alumina surface by cobalt. The stabilization of the XPS intensity ratio for catalysts A2 and A3 corresponds to the formation of rather big crystallites of Co_3O_4 (their size is larger than the XPS analyzed depth), in agreement with the XRD measurements (Table 2). There are, however, some discrepancies between XRD and XPS results for sample G2. Indeed, it contains Co_3O_4 crystallites as big as sample A3 ($d_m \sim 34$ nm), but it is located on the straight line of good dispersion (Figure 7). The origin of this anomaly could be the fact that samples as pellets are ground for the XPS analysis, and the result is averaged between grains initially present at the exterior and inside the pellet. On the other hand, XRD is not sensitive to detect very small particles ($d_m \leq 5$ nm). The SEM observations presented in the next paragraph reveal that, for sample G2, Co_3O_4 is preferably located at the pellet edge. Such a segregation is not evidenced by XPS.

SEM pictures of the Co−alumina oxide catalysts containing about 16 wt % of Co are presented in Figure 8. Cobalt deposited on support A is mainly located at the surface of the grain (Figure 8a). Likewise, the Co_3O_4 concentration is higher at the pellet edges (Figure 8b−d). After impregnation, the catalyst porosity seems to be influenced by both the specific surface area and the macroporosity ($\phi > 0.05$ μm). Apparently, sample porosity is increasing in the order G2 < S2 < C2. Moreover, the initial macroporosity of the support favors the precursor impregnation. In the pellet core of the catalysts C2 and S2, the cobalt oxide dispersion is better than at the pellet edge, in agreement with the XRD crystallite size reported in Table 2. It appears that the technique of impregnation used in this study leads to catalysts with a good mean dispersion. This is also confirmed by the evolution of the XPS intensity ratio with the density of cobalt in the bulk (Figure 7).

The higher concentration of cobalt at the periphery of grains or pellets, proved by SEM observations (Figure 8), is not necessarily bad for catalysis use when diffusion limitation is involved.[38]

Table 3. Distribution of Cobalt Species as a Function of the Reduction Temperature (from Refs 15, 20−22, and 31)

temperature of reduction (K)	$T <$ 570	570 $< T <$ 750	750 $< T <$ 900	900 $< T <$ 1150	$T >$ 1150
Co (metal)	−	X	X	X	X
Co_3O_4	X	−	−	−	−
CoO (from Co_3O_4)		X	−	−	−
surf. Co^{2+} and Co^{3+}	X	X	X	−	−
$CoAl_2O_4$	X	X	X	X	−

Catalysts in the Reduced State. Several steps have been identified through numerous studies dealing with the thermoreduction of Co oxide deposited on alumina.[15,16,21,22,39−41] After calcination, the Co_3O_4 phase with Co^{3+} in the octahedral position (o) and Co^{2+} in the tetrahedral position (t) is generally observed, as we did in the present work. In addition, surface species such as Co^{3+}(o), Co^{2+}(t), and Co^{2+}(o), the proportion of which depends on the interactions between cobalt and the support, are also commonly found. At high calcination temperature (1000 K), an aluminate phase ($CoAl_2O_4$) forms and cannot be reduced below 1150 K. Moreover, it is generally admitted that the smaller the oxide particles are, the more difficult their reduction is, because of stronger interactions with the support.[15,31−37] Species at present reported in the literature, according to the reduction temperature, are summarized in Table 3.

Derivative curves of the A sample series reduction are presented in Figure 9. The reduction of the Co oxide phase(s) is more difficult with a maximum around 600 K for the catalyst with a lower cobalt content (A1). These results confirm the XPS analyses that showed the increase of cobalt−support interaction when the loading decreases.

The influence of the support on the reduction of catalysts containing 15−17 wt % of Co is presented in Figure 10. On these curves, the two steps corresponding to the reduction of (i) Co_3O_4 to CoO and (ii) CoO to metallic Co are clearly identified. The first reduction step (498−623 K) appears to be easy, especially for samples A2 and G2, with a high reduction rate and a reduction temperature range relatively narrow as already observed.[20,35] The second step (623−873 K) happens in different ways for the four solids. For sample A2, the second reduction step appears to be gradual when temperature increases, for samples C2 and S2,

(31) Arnoldy, P.; Moulijn, J. A. *J. Catal.* **1985**, *93*, 38.
(32) Reuel, R. C.; Bartholomew, C. H. *J. Catal.* **1984**, *85*, 63.
(33) Kogelbauer, A.; Goodwin, J. G.; Ouraci, R. *J. Catal.* **1996**, *160*, 125.
(34) Fu, L.; Bartholomew, C. H. *J. Catal.* **1985**, *92*, 376.
(35) Iglesia, E.; Soled, S. L.; Fiato, R. A.; Via, G. H. *J. Catal.* **1993**, *143*, 345.
(36) Johnson, B. G.; Rameswaran, M.; Patil, M. D.; Muralidhar, G.; Bartholomew, C. H. *Catal. Today* **1989**, *6*, 81.
(37) Grimblot, J. *L'analyse de surface des solides par spectroscopies électronique et ionique*; Masson: Paris, 1995.
(38) Iglesia, E.; Soled, S. L.; Baumgartner, J. E.; Reyes, S. C. *J. Catal.* **1995**, *153*, 108.
(39) Soares, R. R.; Frydman, A.; Schmal, M. *Catal. Today* **1993**, *16*, 361.
(40) Moon, S. H.; Yoon, K. E. *Appl. Catal.* **1985**, *16*, 289.
(41) Frydman, A.; Castner, D. G.; Schmal, M.; Campbell, C. T. *J. Catal.* **1995**, *152*, 164.

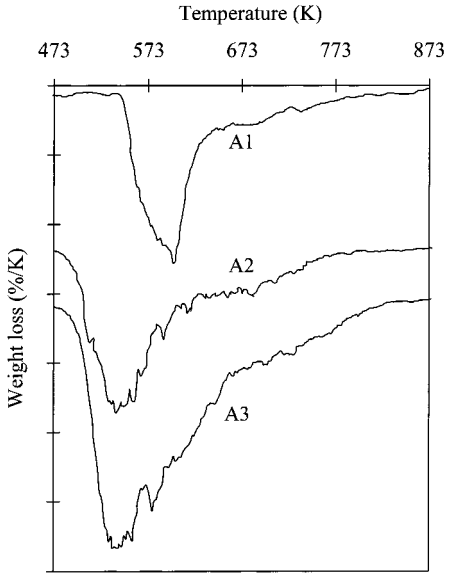

Figure 9. Derivative curves of thermogravimetric reduction of Co−alumina catalysts (series A).

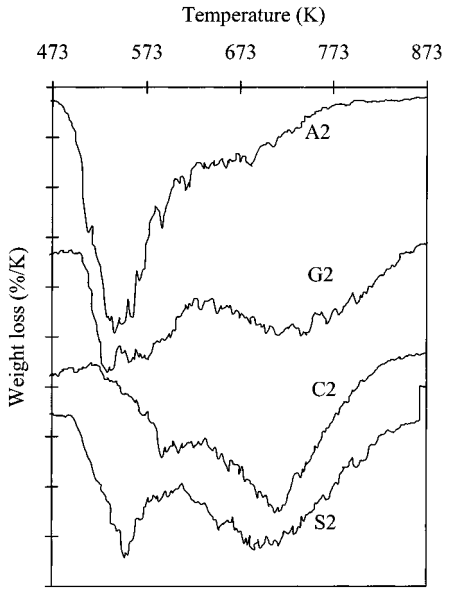

Figure 10. Influence of the support on the Co/Al_2O_3 catalysts reduction.

the reduction rate is important around 700 K, and in the case of catalyst G2, the reduction ranges from 623 to 873 K with a broad maximum at about 730 K.

XRD spectra of catalyst A2 reduced 15 h at different temperatures are shown in Figure 11. The reduction at 498 K leads to the total transformation of the Co_3O_4 phase to CoO. This step has a kinetic limitation because the reduction of Co_3O_4 is complete after 15 h under hydrogen at 498 K, whereas the programmed (1 K min^{-1}) thermoreduction (Figure 10) terminates at around 600 K. On the other hand, the reduction of CoO to metallic Co begins around 623 K and progresses until 773 K where the CoO phase is totally reduced. This second step of reduction is mainly controlled by temperature because the reduction after a 15 h treatment at 623 K is less advanced than after 673 or 723 K.

Thermogravimetric analyses of reduction allow to calculate the reduction extent (R) of the oxide cobalt species. They confirm the influence of the oxide catalyst

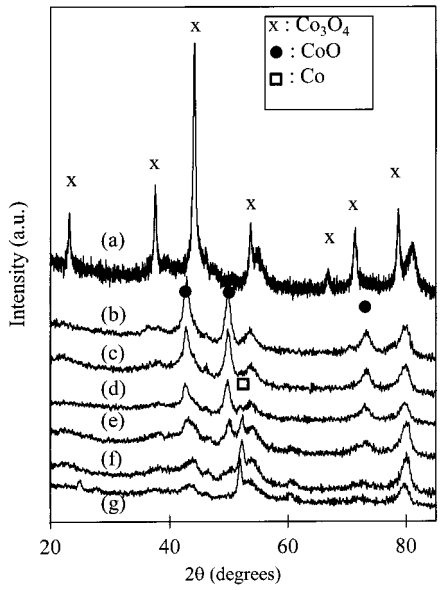

Figure 11. XRD pattern evolution of a Co/Al_2O_3 catalyst (sample A2) during its step by step reduction. After calcination (a) and after reduction at 498 (b), 523 (c), 623 (d), 673 (e), 723 (f), and 773 K (g).

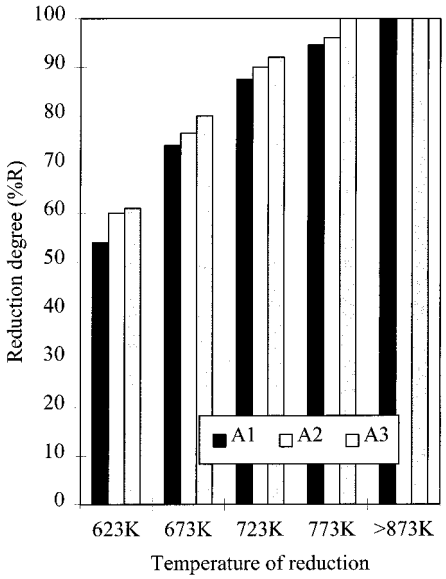

Figure 12. Influence of the cobalt loading on the reduction extent of the Co/Al_2O_3 catalysts.

Table 4. Degree of Cobalt Reduction *R* (%) at 773 K of Selected Co−Alumina Catalysts

catalyst	A2	C2	G2	S2
magnetic measurements	100	67	67	96
thermogravimetry	96	72	62	98

morphology as determined by XRD and SEM on the reduction. The influence of the cobalt loading in series A on R is reported in Figure 12. At each reduction temperature, the reduction extent is more pronounced for the highest cobalt loading, in agreement with the bigger oxide crystallite size (Table 2). The influence of the support on R is presented in Figure 13. The evolution of R confirms the weight loss derivative curves reported in Figure 10. Even at 873 K, samples C2 and G2 are not completely reduced into Co^0. The reduction degree has also been determined by magnetic measurements (Table 4). The results obtained by this technique

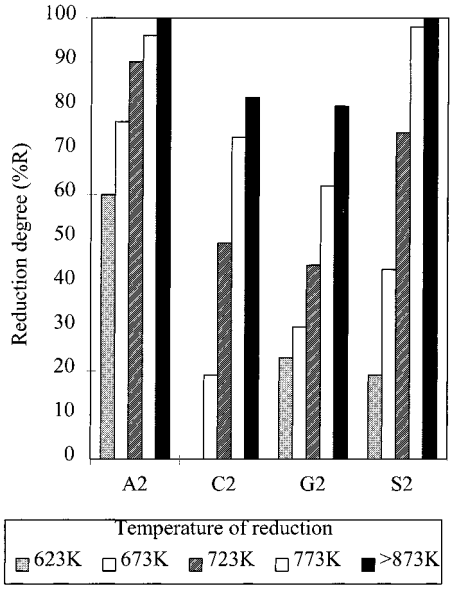

Figure 13. Influence of the support on the reduction extent of Co/Al_2O_3 catalysts.

are in good agreement with the data deduced from the thermogravimetric analyses. After treatment at 773 K, reduction of cobalt is almost complete for catalysts A2 and S2 whereas *R* reaches only 70% for the other samples.

Figure 13 shows that 60% of Co of catalyst A2 is easily reduced while around 20% of cobalt of catalysts G2 and S2 is reduced below 623 K. This cobalt is certainly badly dispersed and localized at the periphery of the grains of the A powder (Figure 8a) and of the pellets (Figure 8b,c). The cobalt species that are reduced from 673 to 873 K are probably well dispersed, and it is especially important in catalysts C2 and S2. At 873 K the reduction of the catalysts G2 and C2 is not complete. The diffusion of the cobalt in alumina with a specific surface area higher than 300 m^2/g probably leads to the formation of an aluminate phase which is not easily reduced below 1150 K.

Conclusion

The thermal decomposition of the cobalt precursor on powder catalysts follows the theoretical steps described in the literature. On catalysts prepared from alumina pellets, this decomposition is initiated by the exothermic impregnation.

The cobalt dispersion is affected by both the support texture and the cobalt content. The mean crystallite size and the surface intensity ratio $(I_{Co}/I_{Al})_{XPS}$ increase with the cobalt loading. The use of alumina pellets with high specific surface area leads to catalysts with a good dispersion in the pellet core. But for higher cobalt content, badly dispersed Co_3O_4 is located at the periphery of the pellets or at the edge of the grains of powder.

The cobalt oxide (Co_3O_4) is reduced in two steps, with intermediate formation of CoO, clearly identified by XRD. Whereas the first step has a kinetic limitation, the second one is more influenced by the temperature of the reduction used. The ease and extent of reduction depend on the strength of interactions between the oxide species and the support. Co^{2+} ions detected by XPS at the catalyst surfaces show the role of these interactions. In the case of catalysts prepared with high specific surface area (>300 $m^2\ g^{-1}$) such interactions are very strong, and the reduction into Co^0 is not complete below 873 K.

Acknowledgment. The authors of the present study thank Mr. Nedez and the Rhône-Poulenc Co. for supplying the supports and information about them, Dr. Chaumette (Kinetics and Catalysis Division-IFP-Rueil Malmaison) for porosity measurements, Mrs. Guelton and Dr. Gengembre (URA CNRS 402 Laboratory—Lille) for thermoreduction, XPS, and BET analyses, and Dr. Martin (IRC—Villeurbane) for the magnetic measurements.

CM981015N